

Positioning Multiple Proteins at the Nanoscale with Electron Beam Cross-Linked Functional Polymers

Karen L. Christman,^{†,§,#} Eric Schopf,^{‡,§} Rebecca M. Broyer,^{†,§} Ronald C. Li,^{†,§}
Yong Chen,^{‡,§} and Heather D. Maynard^{*,†,§}

Department of Chemistry and Biochemistry, Department of Mechanical and Aerospace Engineering, and California NanoSystems Institute, University of California, Los Angeles, 607 Charles E. Young Drive East, Los Angeles, California 90095-1569

Received June 22, 2008; E-mail: maynard@chem.ucla.edu

Abstract: Constructing multicomponent protein structures that match the complexity of those found in nature is essential for the next generation of medical materials. In this report, a versatile method for precisely arranging multicomponent protein nanopatterns in two-dimensional single-layer or three-dimensional multilayer formats using electron beam lithography is described. Eight-arm poly(ethylene glycol)s (PEGs) were modified at the chain ends with either biotin, maleimide, aminoxy, or nitrilotriacetic acid. Analysis by ¹H NMR spectroscopy revealed that the reactions were efficient and that end-group conversions were 91–100%. The polymers were then cross-linked onto Si surfaces using electron beams to form micron-sized patterns of the functional groups. Proteins with biotin binding sites, a free cysteine, an N-terminal α-oxoamide, and a histidine tag, respectively, were then incubated with the substrate in aqueous solutions without the addition of any other reagents. By fluorescence microscopy experiments it was determined that proteins reacted site-specifically with the exposed functional groups to form micropatterns. Multicomponent nanoscale protein patterns were then fabricated. Different PEGs with orthogonal reactivities were sequentially patterned on the same chip. Simultaneous assembly of two different proteins from a mixture of the biomolecules formed the multicomponent two-dimensional patterns. Atomic force microscopy demonstrated that nanometer-sized polymer patterns were formed, and fluorescence microscopy demonstrated that side-by-side patterns of the different proteins were obtained. Moreover, multilayer PEG fabrication produced micron- and nanometer-sized patterns of one functional group on top of the other. Precise three-dimensional arrangements of different proteins were then realized.

Introduction

Many of the desired applications for nanopatterning necessitate that multiple, distinct proteins be conjugated to the same surface with precision. Nanometer features of one type of protein have been successfully fabricated by a number of techniques.¹ These include dip-pen nanolithography (DPN),^{2–4} nanografting,⁵ nanocontact printing,^{6,7} nanoimprint lithography,⁸ and electron

beam (e-beam) lithography.⁹ Self-assembly of particles,¹⁰ polymers,¹¹ and DNA¹² into ordered templates for subsequent protein or peptide attachment has also been employed. Micropatterning of multi-peptides and proteins has been accomplished by a wide variety of methods, including printing, stamping, and photodeprotection.^{13–15} To date, only a few examples of nanopatterning multiple proteins on a single substrate have been reported. DPN has been effectively used to construct arrays of two different proteins by direct writing onto substrates.^{16,17} Likewise, adsorption of multiple antibodies was accomplished using sequential

[†] Department of Chemistry and Biochemistry.

[‡] Department of Mechanical and Aerospace Engineering.

[§] California NanoSystems Institute.

[#] Current address: Department of Bioengineering, University of California, San Diego.

- (1) Christman, K. L.; Enriquez-Rios, V. E.; Maynard, H. D. *Soft Matter* **2006**, *2*, 928–939.
- (2) Lee, K. B.; Park, S. J.; Mirkin, C. A.; Smith, J. C.; Mrksich, M. *Science* **2002**, *295*, 1702–1705.
- (3) Hyun, J.; Ahn, S. J.; Lee, W. K.; Chilkoti, A.; Zauscher, S. *Nano Lett.* **2002**, *2*, 1203–1207.
- (4) Wilson, D. L.; Martin, R.; Hong, S.; Cronin-Golomb, M.; Mirkin, C. A.; Kaplan, D. L. *Proc. Natl. Acad. Sci. U.S.A.* **2001**, *98*, 13660–13664.
- (5) Wadu-Mesthrige, K.; Xu, S.; Amro, N. A.; Liu, G. Y. *Langmuir* **1999**, *15*, 8580–8583.
- (6) Renault, J. P.; Bernard, A.; Bietsch, A.; Michel, B.; Bosshard, H. R.; Delamar, E.; Kreiter, M.; Hecht, B.; Wild, U. P. *J. Phys. Chem. B* **2003**, *107*, 703–711.
- (7) Li, H. W.; Muir, B. V. O.; Fichet, G.; Huck, W. T. S. *Langmuir* **2003**, *19*, 1963–1965.

- (8) Hoff, J. D.; Cheng, L. J.; Meyhofer, E.; Guo, L. J.; Hunt, A. J. *Nano Lett.* **2004**, *4*, 853–857.
- (9) Hong, Y.; Krsko, P.; Libera, M. *Langmuir* **2004**, *20*, 11123–11126.
- (10) Cai, Y.; Ocko, B. M. *Langmuir* **2005**, *21*, 9274–9279.
- (11) Arnold, M.; Cavalcanti-Adam, E. A.; Glass, R.; Blummel, J.; Eck, W.; Kanteleiner, M.; Kessler, H.; Spatz, J. P. *ChemPhysChem* **2004**, *5*, 383–388.
- (12) Yan, H.; Park, S. H.; Finkelstein, G.; Reif, J. H.; LaBean, T. H. *Science* **2003**, *301*, 1882–1884.
- (13) Kane, R. S.; Takayama, S.; Ostuni, E.; Ingber, D. E.; Whitesides, G. M. *Biomaterials* **1999**, *20*, 2363–2376.
- (14) Min, D. H.; Mrksich, M. *Curr. Opin. Chem. Biol.* **2004**, *8*, 554–558.
- (15) Barbulovic-Nad, I.; Lucente, M.; Sun, Y.; Zhang, M. J.; Wheeler, A. R.; Bussmann, M. *Crit. Rev. Biotechnol.* **2006**, *26*, 237–259.
- (16) Lee, K. B.; Lim, J. H.; Mirkin, C. A. *J. Am. Chem. Soc.* **2003**, *125*, 5588–5589.
- (17) Lim, J. H.; Ginger, D. S.; Lee, K. B.; Heo, J.; Nam, J. M.; Mirkin, C. A. *Angew. Chem., Int. Ed.* **2003**, *42*, 2309–2312.

nanografting.¹⁸ A novel vibrational atomic force microscopy (AFM) mode selectively replaced areas of self-assembled protein monolayers with different proteins under mild conditions in a technique called native protein nanolithography.¹⁹ A combination of an elastomeric stamp and a nanotemplate was recently reported for multicomponent protein patterns.²⁰ However, to our knowledge, e-beam lithography has not been employed. This method can not only generate arbitrary protein nanopatterns of different shapes, sizes, and curvatures but also control interfeature spaces and locations precisely. The latter could possibly result in patterns with nanoscale interfeature spacings for heterogeneous patterns. Because of this potential advantage, we sought to determine whether e-beam lithography could be utilized, and here we describe the first multicomponent protein nanopatterns produced by this technique.

Three-dimensional arrangements of multiple proteins also provide entry to a range of sophisticated applications.²¹ For example, intricate, three-dimensional shapes at the micron scale consisting of a single protein have been successfully used to guide neuronal development,²² to trap bacteria,²³ and for bioelectronics.²⁴ Multiprotein structures have been created at the micron scale.²⁵ To our knowledge, constructs with nanoscale components have not yet been realized. We also utilized e-beam lithography to construct the first multicomponent, multilayer heterogeneous protein patterns that range from the micron scale to the nanoscale.

Patterns were prepared by cross-linking an eight-arm poly(ethylene glycol) (PEG) polymer that was modified with one of four protein-reactive moieties: biotin, maleimide, aminoxy, or nickel(II) nitrilotriacetic acid (Ni^{2+} -NTA) (Figure 1a). Each of these groups can conjugate proteins at distinct sites. Biotin is a high-affinity ligand ($K_A \approx 10^{15} \text{ M}^{-1}$) for streptavidin (SAv)²⁶ which is often used as a linker between biotinylated surfaces and biotinylated proteins.³ Maleimides and free cysteines react by Michael addition. Since these residues occur in low abundance in proteins, this reaction is convenient for site-specific immobilization. Aminoxy groups conjugate proteins with reactive carbonyls, chemospecifically forming oxime bonds. Proteins are readily modified by transamination reactions, providing α -oxoamides only at the N-termini²⁷ and a route for site-specific immobilization.²⁸ Ni^{2+} -NTA offers a convenient handle for immobilization of proteins because of the affinity interaction of multiple histidines with the complex.²⁹ Proteins are easily tagged with a polyhistidine sequence at either the C- or N-terminus using recombinant techniques. All of the chosen

polymer end groups provide advantageous conditions for protein immobilization once they are cross-linked to the surface. First, proteins are captured in aqueous solutions at ambient temperature, without the need for additional reagents or activation steps that can lead to protein denaturation. Therefore, sensitive biomolecules prone to denaturation under direct-write conditions may be utilized with this method. Second, immobilization is site-specific; in contrast, physical adsorption or covalent attachment via groups that are abundant on proteins, such as carboxylic acids or amines, often leads to random orientation and loss of bioactivity.

E-beam lithography was employed to prepare the patterns of protein-reactive PEG hydrogels. It is known that when PEG is exposed to focused e-beams, it cross-links to itself and to Si surfaces.^{9,30,31} The process occurs through a radical mechanism similar to that of solution-based radical-mediated cross-linking of PEG.^{32–34} The PEG component not only cross-links to the surface³⁰ but is an opportune choice because it is protein-resistant and therefore typically used as a nonfouling surface.^{35–37} This latter point is important in the production of patterns that resist nonspecific binding while allowing specific protein conjugation via the chosen functionality. In this report, fabrication of the polymer patterns by e-beam lithography, conjugation of the proteins, and characterization by AFM and fluorescence microscopy is described.

Results and Discussion

The end groups of eight-arm PEGs were modified with biotin, maleimide, aminoxy, or NTA, in most cases using commercially available starting materials (see the Supporting Information for experimental procedures). Modification was determined by analysis of the ^1H NMR spectra, and conversions of the end groups were found to be efficient (91, 100, 97, and 100%, respectively). These polymers were then utilized for e-beam cross-linking reactions to form functionalized patterns.

The PEG polymer layer was formed by spin-coating a 2% (w/w) solution in either methanol (maleimide-, aminoxy-, and NTA-PEG) or chloroform (biotin-PEG) onto a Si wafer, and the desired patterns were created using an e-beam lithographic system. Any un-cross-linked polymer was removed by rinsing the samples with methanol and H_2O , producing patterns of functionality (Figure 1a). The technique was first demonstrated for individual end-functional groups with micron-sized features. The e-beam exposure threshold was experimentally determined for each polymer and found to be 60–110 $\mu\text{C}/\text{cm}^2$, with the exception of maleimide-PEG, for which the threshold was 1.1 $\mu\text{C}/\text{cm}^2$. Cross-linking of the PEG occurs by a radical

(18) Zhao, Z.; Banerjee, I. A.; Matsui, H. *J. Am. Chem. Soc.* **2005**, *127*, 8930–8931.

(19) Tinazli, A.; Piehler, J.; Beuttler, M.; Guckenberger, R.; Tampe, R. *Nat. Nanotech.* **2007**, *2*, 220–225.

(20) Coyer, S. R.; Garcia, A. J.; Delamarche, E. *Angew. Chem., Int. Ed.* **2007**, *46*, 6837–6840.

(21) Stephanopoulos, N.; Solis, E. O. P.; Stephanopoulos, G. *AIChE J.* **2005**, *51*, 1858–1869.

(22) Kaehr, B.; Allen, R.; Javier, D. J.; Currie, J.; Shear, J. B. *Proc. Natl. Acad. Sci. U.S.A.* **2004**, *101*, 16104–16108.

(23) Kaehr, B.; Shear, J. B. *J. Am. Chem. Soc.* **2007**, *129*, 1904–1905.

(24) Hill, R. T.; Lyon, J. L.; Allen, R.; Stevenson, K. J.; Shear, J. B. *J. Am. Chem. Soc.* **2005**, *127*, 10707–10711.

(25) Hill, R. T.; Shear, J. B. *Anal. Chem.* **2006**, *78*, 7022–7026.

(26) Weber, P. C.; Ohlendorf, D. H.; Wendoloski, J. J.; Salemme, F. R. *Science* **1989**, *243*, 85–88.

(27) Gilmore, J. M.; Scheck, R. A.; Esser-Kahn, A. P.; Joshi, N. S.; Francis, M. B. *Angew. Chem., Int. Ed.* **2006**, *45*, 5307–5311.

(28) Christman, K. L.; Broeyer, R. M.; Tolstyka, Z. P.; Maynard, H. D. *J. Mater. Chem.* **2007**, *17*, 2021–2027.

(29) Lata, S.; Reichel, A.; Brock, R.; Tampe, R.; Piehler, J. *J. Am. Chem. Soc.* **2005**, *127*, 10205–10215.

(30) Krsko, P.; Sukhishvili, S.; Mansfield, M.; Clancy, R.; Libera, M. *Langmuir* **2003**, *19*, 5618–5625.

(31) Brough, B.; Christman, K. L.; Wong, T. S.; Kolodziej, C. M.; Forbes, J. G.; Wang, K.; Maynard, H. D.; Ho, C. M. *Soft Matter* **2007**, *3*, 541–546.

(32) Sofia, S. J.; Merrill, E. W. *J. Biomed. Mater. Res.* **1998**, *40*, 153–163.

(33) King, P. A.; Ward, J. A. *J. Polym. Sci., Part A: Polym. Chem.* **1970**, *8*, 253–262.

(34) Emami, S. H.; Salovey, R.; Hogen-Esch, T. E. *J. Polym. Sci., Part A: Polym. Chem.* **2002**, *40*, 3021–3026.

(35) Lopina, S. T.; Wu, G.; Merrill, E. W.; Griffith-Cima, L. *Biomaterials* **1996**, *17*, 559–569.

(36) Sofia, S. J.; Premnath, V.; Merrill, E. W. *Macromolecules* **1998**, *31*, 5059–5070.

(37) Prime, K. L.; Whitesides, G. M. *J. Am. Chem. Soc.* **1993**, *115*, 10714–10721.

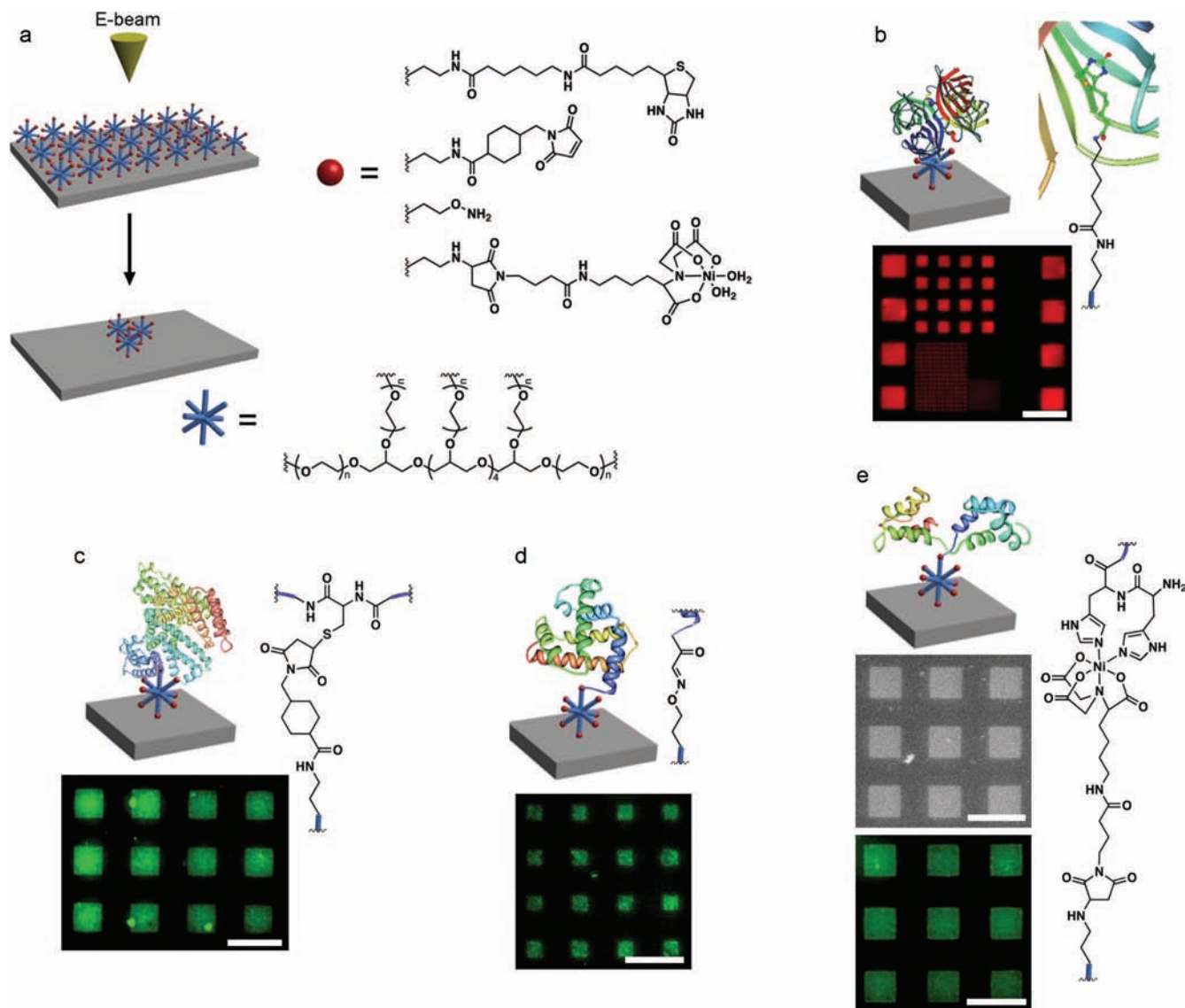


Figure 1. Electron-beam cross-linking of end-functionalized eight-arm PEG polymers for protein patterning. (a) The eight-arm PEGs were spin-coated onto Si wafers and cross-linked to the native oxide using e-beam lithography to generate specific patterns. Each PEG was end-functionalized with one of four protein-reactive handles (biotin, maleimide, aminoxy, or NTA). (b) Alexa Fluor 568 SAV was attached to biotin-PEG patterns through the biotin-SAV interaction. The two features at the bottom-center of the fluorescence image consist of $1\ \mu\text{m}$ and $750\ \text{nm}$ features repeated many times to make up the overall rectangle and square. (c) BSA was immobilized to maleimide-PEG patterns through the sulfhydryl group of the free cysteine in the BSA. (d) Myoglobin that was modified with pyridoxal-5-phosphate to contain an N-terminal α -oxoamide group was attached to aminoxy-PEG patterns through an oxime bond between the aminoxy functionality and the reactive carbonyl at the N-terminus of the modified myoglobin. (e) Histidine-tagged calmodulin was immobilized to Ni^{2+} -NTA-PEG patterns through the nickel-histidine affinity interaction. The original Ni^{2+} -NTA patterns, generated by exposure of the NTA-PEG patterns to nickel(II) chloride hexahydrate, were observed by SEM (upper gray-scale image). All of the proteins with the exception of SAV were labeled with the appropriate antibodies prior to visualization by fluorescence microscopy. Protein structure representations were obtained from the PDB (entries 1SWA, 2BX8, 1WLA, and 1CFD, respectively). Scale bar = $20\ \mu\text{m}$.

mechanism,^{30,38} and thus, it is possible that some of the maleimides participated in this process, lowering the required dose.

Chips were subjected to the appropriate model proteins to produce the desired biomolecule patterns. The proteins were visualized by fluorescence after antibody staining, with the exception of streptavidin, which was already labeled with a dye. Biotin-PEG micropatterns were incubated with Alexa Fluor 568 SAV (Figure 1b); bovine serum albumin (BSA), which contains one free cysteine, was attached to the maleimide-PEG patterns (Figure 1c), and N-terminal α -oxoamide-modified myoglobin was immobilized to aminoxy-PEG designs (Figure 1d). The latter protein was formed by an N-terminal-specific transamination reaction using a recently reported procedure²⁷ (see

the Supporting Information for experimental details). To create the Ni^{2+} -NTA-PEG patterns, NTA-PEG features were first generated, and then Ni^{2+} was chelated. The metal-chelated surface was characterized by scanning electron microscopy (SEM), which demonstrated that the Ni^{2+} -NTA-PEG was patterned as expected (Figure 1e, top). A histidine-tagged calmodulin was subsequently immobilized (Figure 1e, bottom). In every case, fluorescence was located only on the patterns (Figure 1b–e).

Each surface was also subjected to control experiments in which the protein handle was consumed by presaturation with a compound containing the respective functional group, except in the case of Ni^{2+} -NTA-PEG, where no Ni^{2+} was present in the control. No fluorescence was detected for the biotin-,

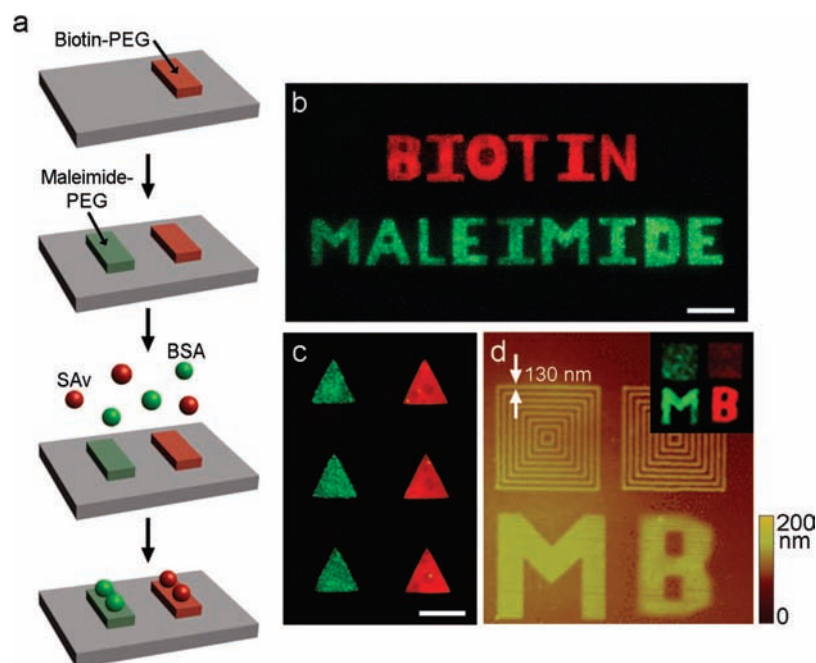


Figure 2. Dual-protein patterning. (a) Biotin-PEG and maleimide-PEG are cross-linked next to each other using e-beam lithography. BSA, which conjugates to the maleimide-PEG, and SAV, which binds to the biotin-PEG, are attached simultaneously from the same solution. BSA is visualized using the appropriate antibodies. (b, c) Fluorescence overlays demonstrating attachment of the two proteins to microscale patterns (scale bar = 10 μm). (d) Nanoscale patterns of the two functionalized PEGs with line widths of 130 nm are visible. “M” and “B” are written below the patterns to denote the respective PEGs. The inset displays a fluorescence overlay of the nanoscale patterns with attached BSA and SAV.

aminoxy-, and Ni^{2+} -NTA-PEG controls, and little fluorescence was observed for maleimide-PEG. This demonstrated that protein immobilization was a result of the desired chemistry rather than random adsorption on the functionalized patterns. The slight fluorescence that was observed for maleimide-PEG was eliminated when the BSA was directly labeled with the fluorophore (data not shown); it was therefore attributed to nonspecific binding of the antibodies, which may have been caused by the presence of free cysteines.³⁹ Taken together, these results indicated site-specific attachment of the proteins to the functional groups, which is important for fabrication of bioactive features. In addition, undesirable nonspecific protein adsorption outside of the patterns was minimal (signal-to-noise ratios are provided in the Supporting Information). This is important for the elimination of large background signals for the application of these materials and is likely due to the low concentrations of proteins and short contact times utilized in the staining of the surface.⁵ If required for a particular application, nonspecific adsorption could be further minimized by cross-linking the star PEGs onto Si precoated with a thin, nonfunctionalized PEG layer.^{9,31}

With this e-beam-induced cross-linking strategy, it is feasible to pattern more than one type of eight-arm PEG on the surface. Each of the described end groups interacts with proteins via a different mechanism. Therefore, immobilization of multiple proteins directed by the different functional groups is possible (Figure 2a). To demonstrate this, we first patterned the biotin-PEG on Si wafers at the micron scale. After removal of un-cross-linked polymer, the maleimide-PEG features were subsequently fabricated on the same chip next to the biotin

patterns. Next, the samples were treated by incubation with a solution containing both Alexa Fluor 568 SAV and BSA followed by antibody staining. Red fluorescence was observed at locations of the biotin-PEG patterns, while green fluorescence was observed at the maleimide-PEG patterns (see the fluorescence overlays in Figure 2b,c). This demonstrated that the proteins were arrayed as directed by the functional groups on the surface with good specificity (individual green and red fluorescent channels are provided in the Supporting Information). Interestingly, the proteins were arrayed simultaneously from a mixture of the biomolecules; although this result is not critical, it showed that sequential immobilizations may not be necessary. The results also illustrated that a variety of designs, such as letters and triangles, can be produced, which is an advantage of e-beam lithography.

E-beam lithography can produce high-resolution nanostructures; therefore, nanoscale patterning of both proteins was next demonstrated. Concentric squares of biotin and maleimide were sequentially fabricated side by side. Below each, a micron-sized letter indicating either maleimide (M) or biotin (B) was also fabricated to allow for easy identification of the different functional nanopatterns. The AFM images in Figure 2d display 130 nm wide nanoscale patterns of the two functionalized PEGs aligned next to each other. The concentric squares allowed visualization by standard fluorescence. Again, SAV and BSA were simultaneously immobilized, and the corresponding red and green fluorescence were observed on both the micron-sized letters and nanoscale patterns (fluorescence overlay, Figure 2d, inset). This confirmed the self-sorting of the proteins (individual green and red fluorescent channels are provided in the Supporting Information). These results demonstrated that the original functional groups directed the formation of multicomponent protein patterns with nanosized features.

(38) Merrill, E. W.; Dennison, K. A.; Sung, C. *Biomaterials* **1993**, *14*, 1117–1126.

(39) Gevondyan, N. M.; Volynskaia, A. M.; Gevondyan, V. S. *Biochemistry (Moscow)* **2006**, *71*, 279–284.

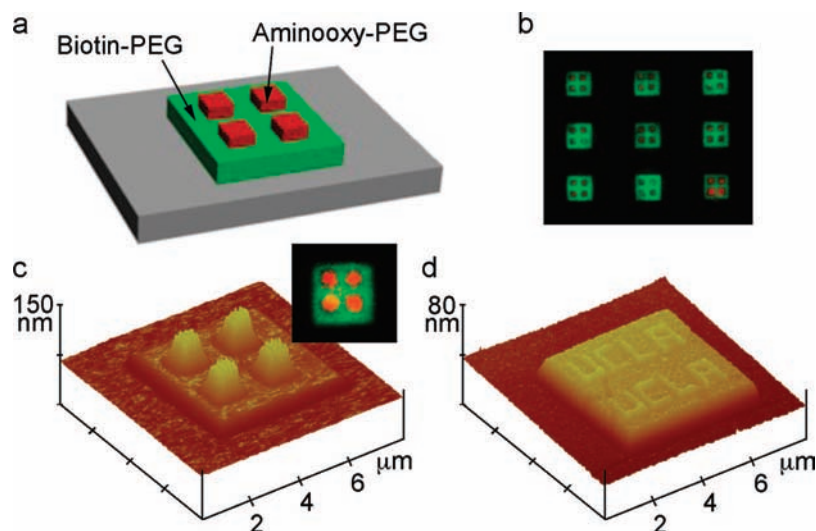


Figure 3. Multilayer, multicomponent biostructures. (a) Schematic showing that biotin-PEG is first cross-linked to the native oxide of a Si wafer, after which aminoxy-PEG patterns are cross-linked on top of the original biotin-PEG patterns. (b, c) Four $1 \times 1 \mu\text{m}$ aminoxy-PEG patterns are cross-linked on top of base $5 \times 5 \mu\text{m}$ biotin-PEG patterns. (b) Fluorescence after incubating a 3×3 grid of multicomponent structures with green fluorescent SAV, which binds to the biotin-PEG, and red fluorescent antibody-stained N-terminal α -oxoamide myoglobin, which binds to the aminoxy patterns. The inset in (c) is one of the features in (b). (c, d) Three-dimensional representations of the AFM height images acquired in tapping mode. (d) Aminoxy “UCLA” pattern with 250 nm wide lines on a $5 \times 5 \mu\text{m}$ biotin-PEG pattern base.

Patterning multiple proteins in multiple layers is also possible because PEG can be induced to cross-link to itself.^{9,31} To demonstrate this, micron- and nanometer-sized features of aminoxy-PEG were patterned on top of a micron-sized biotin-PEG pattern (Figure 3a). This was accomplished by cross-linking the biotin-PEG, washing, aligning, and then cross-linking the aminoxy-PEG. Through the use of this approach, four $1 \mu\text{m}$ features and the characters “UCLA” with 250 nm line widths consisting of aminoxy-PEG were fabricated on top of $5 \times 5 \mu\text{m}$ biotin-PEG patterns. AFM images taken in tapping mode revealed that the underlying biotin-PEG was not ablated but rather that the aminoxy-PEG was cross-linked on top of the original patterns, creating 3D topographical structures (Figure 3c,d). To confirm protein immobilization on these multilayer patterns, the samples were treated by incubation with a solution containing both Alexa Fluor 488 SAV and N-terminal α -oxoamide myoglobin followed by Alexa Fluor 633 antibody staining. Although the nanoscale “UCLA” could not be resolved with conventional fluorescence microscopy, the $1 \mu\text{m}$ patterns were observed. A fluorescent image overlay of a 3×3 grid of this multilayer pattern (Figure 3b; individual channels provided in the Supporting Information) indicated that the green fluorescent SAV was immobilized on the bottom biotin-PEG pattern and that myoglobin was localized on the top aminoxy patterns.

To further investigate the scope of this methodology, micron- and nanometer-sized features of maleimide-PEG were patterned on top of a micron-sized biotin-PEG pattern (Figure 4a). With this approach, four $1 \mu\text{m}$, sixteen 500 nm, and sixteen 250 nm features of maleimide-PEG on top of $5 \times 5 \mu\text{m}$ biotin-PEG patterns were fabricated. AFM images taken in tapping mode again revealed that the underlying biotin-PEG was not ablated and that the maleimide-PEG was cross-linked on top of the original patterns, creating topographical structures (Figure 4b–d). To confirm protein immobilization on these multilayer patterns, the samples were incubated with a solution of Alexa Fluor 568 SAV and BSA. Again, although the nanoscale features could not be resolved, a fluorescent image overlay of the $1 \mu\text{m}$ pattern (inset of Figure 4b) indicated that the red fluorescent SAV was immobilized on the bottom biotin-PEG pattern and

that BSA was localized on the top maleimide patterns. These results suggested that other patterns and functional groups can be achieved utilizing this methodology.

Finally, a tripattern with both maleimide-PEG and aminoxy-PEG on top of biotin-PEG was fabricated. The maleimide and aminoxy were purposely cross-linked using doses that achieved different heights³⁰ in order to provide easy visual identification. AFM images revealed that this additional combination of functionalized PEGs could also be cross-linked into three-dimensional patterns. Figure 5 displays four $1 \times 1 \mu\text{m}$ patterns, two maleimide-PEG and two aminoxy-PEG, on top of a $5 \times 5 \mu\text{m}$ biotin-PEG pattern. The surface was treated by incubation with Alexa Fluor 350 SAV, Alexa Fluor 555 BSA, and α -oxoamide myoglobin followed by Alexa Fluor 488 antibody staining. Remarkably, fluorescence revealed that all three proteins had been patterned (Figure 5b, inset).

Conclusions

We report a versatile approach for fabricating nanopatterns of multiple proteins using e-beam lithography that provides ready access to both single-layer and multilayer formats. Cross-linking of PEG-based polymers with protein-reactive end groups provides a tool for generating features in a variety of designs. Proteins react site-specifically under mild, aqueous conditions. Side-by-side patterns of PEG hydrogels with reactive groups direct the binding of different proteins from a mixture of the biomolecules. There exist many handles and ligands for attachment of proteins to polymers,⁴⁰ and this approach should be directly applicable for immobilizing additional combinations of proteins. Furthermore, this technique is powerful for creating structures containing multiplexed biomolecules in three-dimensional multilayer formats. This offers exciting possibilities for constructing topographically interesting biomolecular systems for site-isolation enzyme cascades⁴¹ and “nanoscale

(40) Heredia, K. L.; Maynard, H. D. *Org. Biomol. Chem.* **2007**, *5*, 45–53.

(41) Vriezema, D. M.; Garcia, P. M. L.; Oltra, N. S.; Hatzakis, N. S.; Kuiper, S. M.; Nolte, R. J. M.; Rowan, A. E.; van Hest, J. C. M. *Angew. Chem., Int. Ed.* **2007**, *46*, 7378–7382.

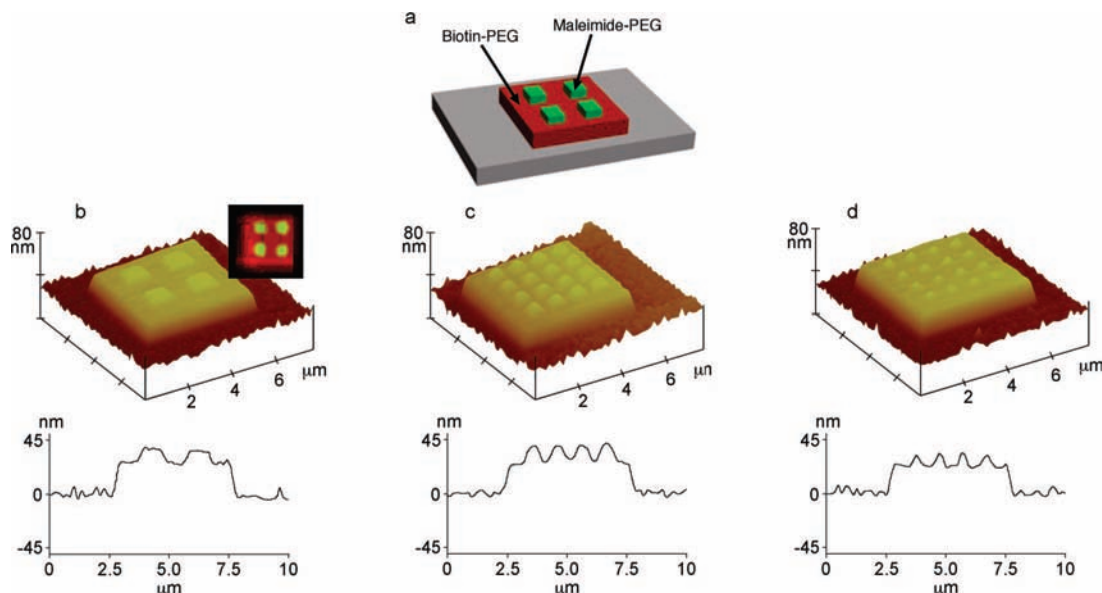


Figure 4. Additional multilayer, multicomponent biostructures. (a) Schematic showing that biotin-PEG is first cross-linked to the native oxide of a Si wafer, after which maleimide-PEG patterns are cross-linked on top of the original biotin-PEG patterns. (b–d) AFM images acquired in tapping mode: (top) three-dimensional representations of the height images; (bottom) graphs showing the height profiles. All of the images contain a base $5 \times 5 \mu\text{m}$ biotin-PEG pattern, and (b) four $1 \mu\text{m}$ wide, (c) sixteen 500 nm wide, and (d) sixteen 250 nm wide maleimide-PEG patterns are cross-linked on top of the biotin-PEG. The inset in (b) displays fluorescence after incubation of the sample with red fluorescent SAV, which binds to the biotin-PEG, and green fluorescent antibody-stained BSA, which binds to the maleimide-PEG patterns.

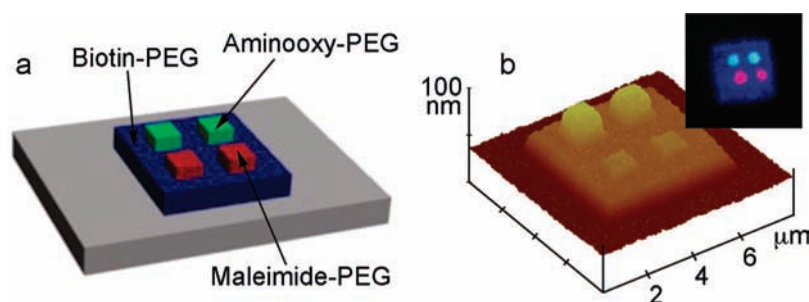


Figure 5. Tricomponent biostructures. (a) Schematic showing that $5 \mu\text{m}$ wide biotin-PEG is first cross-linked to the native oxide of a Si wafer, after which two $1 \mu\text{m}$ wide maleimide-PEG and two $1 \mu\text{m}$ wide aminoxy-PEG patterns are then cross-linked on top of the original biotin-PEG pattern. (b) Three-dimensional representation of the AFM height images of the aminoxy-maleimide-biotin pattern. Inset: overlay image of a blue fluorescent SAV on the biotin-PEG, a green fluorescent antibody-stained α -oxoamide myoglobin, and a red fluorescent BSA.

factories”²¹ in addition to generating materials that match complex structures found in nature, such as protein-signaling assemblies and viral capsids.⁴² Also, it is known that both micron and nanometer chemical and topographical cues are critical for cell adhesion.^{11,22,43–45} The methodology described here is useful for generating surfaces where both chemistry and topography are spatially controlled. Thus, it can be envisioned that by patterning extracellular matrix-derived signals, the surfaces will aid in the study of the intricate relationship between subcellular chemical and topographical cues that can lead to differences in adhesion, proliferation, and protein expression or differentiation. This information would be valuable for

understanding how to control cell behavior and for creating the next generation of biomaterials. We are currently exploring these possibilities.

Experimental Section

Materials. Si chips were cleaned by exposure to piranha (3:1 $\text{H}_2\text{SO}_4/\text{H}_2\text{O}_2$, **caution!**). The chips were then rinsed with and stored in Millipore H_2O . Immediately before spin-coating, Si wafers were further cleaned by rinsing with acetone, methanol, isopropyl alcohol, and Millipore H_2O for $\sim 10 \text{ s}$ each and then dried with a stream of air. For multicomponent PEGs, gold features were fabricated on the Si chips prior to PEG spin-coating and writing. Chips were cleaned in piranha and patterned via standard photolithography procedures. Next, 10 nm of titanium followed by 300 nm of gold was deposited on the chips by metal evaporation, and patterns were developed by lift-off. This resulted in gold squares and lines that were used in later steps solely as reference markers to align the e-beam patterns to a fixed location on the chip in order to ensure alignment precision when patterning multiple PEGs.

Methods. Samples were visualized with fluorescence microscopy using a Zeiss Axiovert 200 fluorescent microscope equipped with an AxioCam MRm monochrome camera or a Zeiss Axiovert 200

(42) Steinmetz, N. F.; Evans, D. J. *Org. Biomol. Chem.* **2007**, *5*, 2891–2902.

(43) Senaratne, W.; Sengupta, P.; Jakubek, V.; Holowka, D.; Ober, C. K.; Baird, B. *J. Am. Chem. Soc.* **2006**, *128*, 5594–5595.

(44) Walter, N.; Selhuber, C.; Kessler, H.; Spatz, J. P. *Nano Lett.* **2006**, *6*, 398–402.

(45) Craighead, H. G.; James, C. D.; Turner, A. M. P. *Curr. Opin. Solid State Mater. Sci.* **2001**, *5*, 177–184.

M microscope equipped with a Hamamatsu C4742–95 monochrome camera, and pictures were acquired and processed using AxioVision LE 4.1. The 3D images and nanoscale side-by-side patterns were taken with a 40X objective. AFM images were collected on dry samples using a Dimension 3100 atomic force microscope (Digital Instruments) in tapping mode (silicon cantilever, spring constant ≈ 40 N/m, tip radius ≤ 10 nm, scan rate = 1.5 Hz) and processed and analyzed using NanoScope IIIa version 5.30r1 (Digital Instruments). SEM samples were mounted to the sample holder using carbon tape and imaged with no additional processing on a JEOL JSM-6700F field-emission scanning electron microscope. An accelerating voltage of 10 kV, a probe current of 10 pA, and a working distance of 8 mm were used.

Pattern Formation. The basic scheme for creating all of the end-functionalized polymer patterns was as follows: A 2% (w/w) PEG solution in either methanol (maleimide–, aminoxy–, and NTA–PEG) or chloroform⁴⁶ (biotin–PEG) was spin-coated onto a cleaned Si chip at 3000 rpm for 20 s. The chips were then used directly without any drying or baking steps. Specific patterns of polymer were cross-linked to the native oxide of the Si using a JC Nabit e-beam lithographic system (Nanometer Pattern Generation System, version 9.0) modified from a JEOL 5910 scanning electron microscope. An accelerating voltage of 30 kV was used, with a beam current of ~ 4.5 pA. Biotin–, maleimide–, aminoxy–, and NTA–PEG micropatterns were generated using minimum e-beam doses of 110, 1.1, 60, and 90 $\mu\text{C}/\text{cm}^2$, respectively. The biotin–, aminoxy–, and maleimide–PEG nanopatterns were generated with line doses of 3, 0.5, and 0.03 nC/cm, respectively. After exposure, any un-cross-linked polymer was removed by rinsing the samples in methanol for 5–10 s followed by rinsing in Millipore H₂O for 5–10 s and drying with a stream of N₂. Ni²⁺-NTA–PEG was generated by dipping the NTA–PEG patterns in a solution of nickel(II) chloride hexahydrate (200 mg/mL in Millipore H₂O) for 20 min, rinsing with Millipore H₂O, and drying with a stream of air. For side-by-side and multilayer patterns, biotin features were first generated by the process described above. After the un-cross-linked biotin–PEG was removed by rinsing with methanol, a layer of the second aminoxy–PEG or maleimide–PEG was spin-coated onto the same chip. The chips were then aligned utilizing gold features that had been prefabricated onto the chip, and the second PEG patterns were cross-linked as described above, either next to or on top of the original biotin–PEG patterns. A wash step removed any unreacted PEG. For the tripatterned chip, aminoxy–PEG was cross-linked, followed by maleimide–PEG.

Pattern Visualization. Micron-Sized Patterns. Individual biotin–, maleimide–, aminoxy–, and Ni²⁺-NTA–PEG patterns were incubated with Alexa Fluor 568 SA_v [5 $\mu\text{g}/\text{mL}$ in phosphate buffered saline (PBS)], BSA (10 $\mu\text{g}/\text{mL}$ in PBS), α -oxoamide-myoglobin (10 $\mu\text{g}/\text{mL}$ in phosphate buffer, 25 mM, pH 6.5), and His-tagged calmodulin (5 $\mu\text{g}/\text{mL}$ in PBS), respectively, for 1 h. With the exception of SA_v, bound proteins were visualized by

staining with a primary antibody for 1 h in PBS followed by a secondary antibody for 30 min in PBS. A concentration of 20 $\mu\text{g}/\text{mL}$ was used for all secondary antibodies. BSA was labeled with a sheep anti-BSA antibody (20 $\mu\text{g}/\text{mL}$) and an Alexa Fluor 488 antisheep secondary antibody. Myoglobin was stained with a goat antimyoglobin (equine myocardium) antibody (1:50 dilution) and then an Alexa Fluor 488 antigoat secondary antibody. A mouse anticalmodulin antibody (200 $\mu\text{g}/\text{mL}$) and an Alexa Fluor 488 antimouse secondary antibody were used to label calmodulin. Samples were rinsed with PBS for 10 s after each incubation step. As controls, SA_v, BSA, and α -oxoamide-myoglobin were incubated with an excess of biotin, maleimide, and *O*-methoxyamine hydrochloride, respectively, for 1 h prior to addition to the patterned substrates. As a control for nickel Ni²⁺-NTA–PEG, NTA–PEG samples were incubated with calmodulin in the absence of Ni²⁺.

Side-by-Side Patterns. Substrates were incubated with a solution containing both Alexa Fluor 568 SA_v (5 $\mu\text{g}/\text{mL}$) and BSA (10 $\mu\text{g}/\text{mL}$) in PBS for 1 h. BSA was stained with sheep anti-BSA antibody and Alexa Fluor 488 antisheep secondary antibody as described above.

Staining of Aminoxy on Biotin. The substrate was incubated with a solution containing Alexa Fluor 568 SA_v (5 $\mu\text{g}/\text{mL}$) in PBS for 1 h. In PBS (pH 6.5), α -oxoamide myoglobin (10 $\mu\text{g}/\text{mL}$) was incubated with the aminoxy patterns for 1 h. The myoglobin was stained with goat antimyoglobin (equine myocardium) antibody (10 $\mu\text{g}/\text{mL}$) followed by Alexa Fluor 633 antigoat secondary antibody (1 $\mu\text{g}/\text{mL}$) as described above.

Staining of Maleimide on Biotin. Same as above for the side-by-side patterns.

Staining of Aminoxy and Maleimide on Biotin. The substrate was incubated with a solution containing α -oxoamide myoglobin (10 $\mu\text{g}/\text{mL}$), Alexa Fluor 555 BSA (10 $\mu\text{g}/\text{mL}$), and Alexa Fluor 350 SA_v (10 $\mu\text{g}/\text{mL}$) in SuperBlock Blocking Buffer (pH 6.2) for 1 h. The chips were then washed with SuperBlock Blocking Buffer, and the myoglobin was stained with goat antimyoglobin (equine myocardium) antibody (10 $\mu\text{g}/\text{mL}$) and Alexa Fluor 488 antigoat secondary antibody (5 $\mu\text{g}/\text{mL}$) as described above.

Acknowledgment. This research was supported by the National Science Foundation (CHE-0645793) and through SINAM (DMI-0327077). K.L.C. thanks the NIH NHLBI for an NRSA Postdoctoral Fellowship. H.D.M. appreciates the Alfred P. Sloan Foundation Research Fellowship and thanks Amgen (New Faculty Award) for additional funding. Christopher M. Kolodziej is thanked for assistance with SEM and Zachary Tolstyka for modifying the myoglobin.

Supporting Information Available: Reagent and protein sources, polymer synthesis, myoglobin modification, and single-channel fluorescence images. This material is available free of charge via the Internet at <http://pubs.acs.org>.

JA804767J

(46) The polymer film formed from biotin–PEG in methanol was not uniform. It was for this reason that biotin–PEG was spin-coated from chloroform.